Corrosion Behaviour of Substoichiometric TiNx Films Produced by DC Magnetron Sputtering

E. Ariza[1], L. A. Rocha[1,2], F. Vaz[3], L. Rebouta[3], J. Ferreira[3], E. Alves[4], Ph. Goudeau[5], J. P. Rivière[5]

[1]CIICS – Research Centre on Interfaces and Surfaces Performance, University of Minho, Campus de Azurém, 4800-058 Guimarães – PORTUGAL.
Phone: +351 253 510220, Fax: +351 253 516007. e-mail: edith@dem.uminho.pt

[2] DEM –Mechanical Engineering Department, University of Minho, Campus de Azurém, 4800-058 Guimarães – PORTUGAL

[3] Dept. Physics, University of Minho, Campus de Azurém, 4800-058 Guimarães – PORTUGAL

[4]ITN, Physics Department, E.N.10, 2685 Sacavém, PORTUGAL

[5]Laboratoire de Métallurgie Physique, Université de Poitiers, 86960 Futuroscope, FRANCE

Keywords: TiN coatings, reactive magnetron sputtering, corrosion resistance, EIS.

Abstract. The present work describes the corrosion behaviour of substoichiometric TiN_x films obtained by dc reactive magnetron sputtering. The coatings thickness ranged from 1.7 to 4.2 μm and the nitrogen content varied between 0 and 55 at. %. According to structural characterization by XRD, the films revealed a hexagonal α-Ti phase with a strong [002] orientation for low nitrogen contents. For nitrogen contents of 20% and 30%, the ε-Ti_2N phase appears with a [200] orientation and further increasing of nitrogen content showed that the δ-TiN phase was dominant.
Potentiodynamic polarisation and Electrochemical Impedance Spectroscopy (EIS) techniques were used to study the corrosion properties of TiN_x films when immersed in artificial sweat solutions. Results of potentiodynamic polarisation tests showed that all films have a high corrosion resistance reflected by corrosion current densities values lower than 0.7μA/cm^2. Also, EIS tests corroborated the results obtained in the polarisation tests, showing that films containing low percentages of nitrogen (less than 8 %) reveal the best corrosion resistance. Further increases in nitrogen content lead to a decrease in corrosion resistance. An exception to this behaviour was found for the film, with 30 % N. This sample presents an excellent corrosion resistance which increases with the immersion time. Higher nitrogen contents (52 and 55 %) promote a relative increase in the corrosion resistance when compared with 45 and 50 at % films, but never reaching values obtained for nitrogen contents lower than 30 % at.

Introduction

Stoichiometric titanium nitride (TiN) is actually one of the most important technological coating material, not only because of its excellent tribological properties but also due to a good chemical stability. It is certainly, in tribological terms, the most explored hard thin film material and most extensively used in industry. It is used in a wide range of applications, which range from protective material for machine parts and cutting tools [1] to diffusion barriers in semiconductor technology [2]. In the last decades there has been an increasing interest in elucidating the mechanisms, which lead to thin-film property modification caused by the so-called substoichiometric condition of TiNx films [3-5]. In recent years, properties of substoichiometric titanium nitride (TiN_x) have been studied by relatively few researchers considering only basic properties such as hardness, phase composition or lattice distortion [6-8]. All these investigations focused mainly on the δ-TiN-phase, whereas little attention was paid to the properties of α-TiN and ε-Ti_2N phases, and especially to the corrosion properties of these films. In this paper, the corrosion behaviour of substoichiometric TiN_x films, remarking the influence of nitrogen content, will be described.

Materials and methods

Specimen preparation. The TiN_x films were deposited by reactive dc magnetron sputtering, from a high purity Ti target onto polished high-speed steel (AISI M2). The depositions were carried out in a "home-made" apparatus under Ar/N_2 atmosphere [9]. Prior to deposition, substrates were *ex situ* ultrasonically cleaned and *in situ* sputter etched for 15 min in a pure Ar atmosphere, using a pulsed power supply: I ≈ 0.35 A; V ≈ 300 V; *f* = 200 kHz. A pure titanium adhesion layer with a thickness of ~ 0.40 μm was deposited on the substrate prior to coating deposition. Substrates were dc biased with a potential of –70 V and the temperature reached the value of about 250 ºC during depositions. The partial pressure of nitrogen was varied from 0 to $3x10^{-2}$ Pa, in order to control the nitrogen content in the coatings (0 to 55 at %).

Composition and hardness determination. X-ray diffraction (XRD) diffractograms have been recorded using a conventional SIEMENS D5000 diffractometer. Coating hardness was determined from the loading and unloading curves, carried out with an ultra low load depth sensing nanoindenter.

Electrochemical Test. The electrochemical tests were performed at room temperature in an artificial sweat solution (pH= 4.57) containing 0.75 g NaCl; 0.12 g KCl; 0.1 g CH_4N_2O (urea); 0.1 ml $C_3H_6O_3$ (lactic acid) and distilled water up to 100 ml. Just before being tested all samples were sonicated in ethanol (15 min) and distilled water (10 min) and finally dried. The same cleaning treatment was carried out for all samples in order to analyse the surface films after corrosion test. All measurements were conduced in a standard three-electrode cell. A saturated calomel electrode (SCE) was used for the potential measurements. A PGP201 Potentiostat/Galvanostat (Radiometer Denmark), controlled by the VoltaMaster software, was used to carried out the polarization measurements and a Voltalab PGZ100 Potentiostat (Radiometer Analytical), controlled by the VoltaMaster-4 software, was used for the EIS measurements. Prior to polarization tests the open circuit potential (OCP) was monitored during 1 h, after which the samples were anodically polarised from -800 mV up to 2000 mV at a scan rate of 2 $mV.s^{-1}$. The EIS measurements were performed in the frequency range from 100 KHz to 10 mHz, with a AC sine wave amplitude of 10 mV applied to the electrode at its corrosion potential. EIS measurements were performed at increased immersion times (60 min, 1, 2 and 3 days). For EIS data simulation the ZView2 software was used.

Results and Discussion

Structural and hardness characterization. In Fig. 1 XRD patterns of the films as a function of the nitrogen content are presented. It can be observed that for low nitrogen contents, the films revealed a hexagonal α-Ti phase with a strong [002] orientation. For nitrogen contents of 20% and 30%, the ε-Ti_2N phase appears with a [200] orientation and further increasing of nitrogen content showed that the δ-TiN phase was dominant.

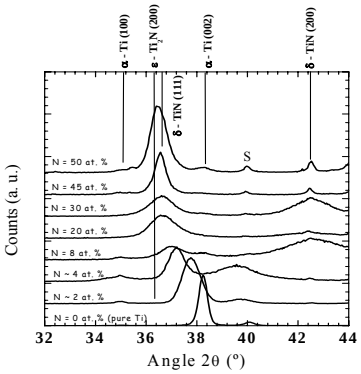

Fig. 1. XRD patterns of TiN_x films as a function of the nitrogen content.

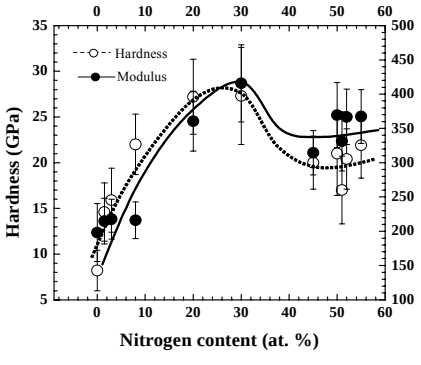

Fig. 2. Hardness and Young's modulus of TiN_x films as a function of the nitrogen content

Although the presence of the ε-Ti_2N phase can not be clearly identified due to the influence of the diffraction peak corresponding to the {111} planes of the δ-TiN phase, its existence is predicted by the Ti-N phase diagram, being reported by others authors [10, 11, 12]. Also, it can be observed that in the case of the

TiNx with 20 and 30 at % N, the diffraction peaks become rather broad indicating that grains of very small sizes are developed. The same behaviour has been reported by *Yang et al.* [11] whom refer that the structure of the film tend to became thinner as the ε-Ti_2N phase becomes dominant. This decrease in grain size is also responsible for the smoothening of the columnar structure which was also reported by *Kohlscheen et al.* [10] in the ε-Ti_2N/δ-TiN transition regime of TiN films. As a consequence, the surface roughness of these samples becomes very smooth, as it is the case of the 30 at% N film.

The evolution of the film hardness as a function of nitrogen content is presented in Fig. 2. It can be observed that a maximum hardness of ca. 27 GPa is obtained in the film containing 30% N. Further increase in the nitrogen content causes a decrease in hardness for values around 20 GPa. The initial hardening effect (low N content) is generally attributed to the distortion of the α-Ti lattice, while the maximum value is coincident with the presence of ε-Ti_2N phase. In fact, the hardening effect provided by this phase has been studied by *Huang et al.* [12]. According to these authors, the presence of ε-Ti_2N phase with a thin structure is responsible for a very high hardness (ca. 30 GPa), when compared with the 21–23 GPa of hardness characteristic of films with a high content of δ-TiN.

Corrosion Behavior. In Fig. 3, the range of variation of the polarisation curves representative of the behaviour of each film is presented. For comparison, the polarisation behaviour of the substrate is also plotted in the Figure. As it can be observed, most TiNx films appear to present two separate passive regions. However, as shown in Fig. 3, the passive current densities in the samples with less than 2 at % of N are one to three times lower in magnitude than that measured in the samples with higher amounts of nitrogen. For this last group of samples, an increase in nitrogen content seems to be related with an increase in the passive current densities. Additionally, as shown in the Figure, the film with 30% N presents passive current densities similar to the samples with very low N content. In this sample, the distinction between the two passive plateaus is not very clear.

The evolution of the corrosion current density (i_{corr}) and of the film thickness with the amount of nitrogen is presented in Fig. 4. A first remark refers to the fact that the corrosion current densities of all films are relatively low in magnitude, being in all cases inferior to 0.7 μA.cm^{-2}. This is a strong indication of the strong protective characteristics of TiNx films when applied to steel, which show a corrosion current density of 48.9 μA.cm^{-2}. An increase in the N content seems to give rise to an increase in the corrosion current densities. However, two different trends may be observed in the graph, with the samples with 30, 52 and 55 % N presenting i_{corr} values much lower than the samples with 20, 45 and 50%. Also, as it can be seen in the graph, the variation in film thickness does not explain by itself the variations in corrosion current, indicating that other parameters, such as composition and structure, play an important role in the corrosion behaviour.

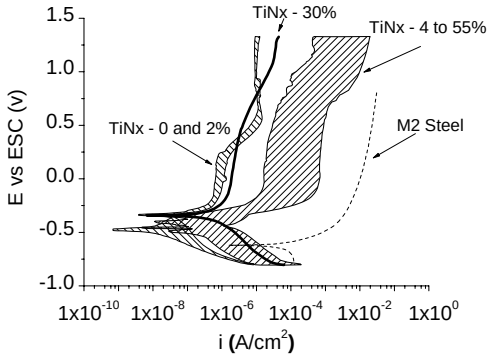

Fig. 3. Polarisation anodic curves obtained for TiNx films immersed in artificial sweat solution.

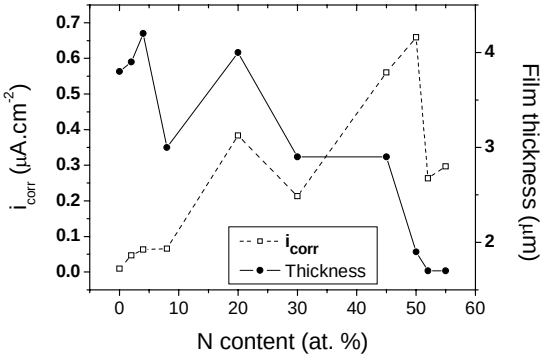

Fig. 4. Influence of the nitrogen content on the corrosion current density and film thickness.

In Fig. 5 SEM micrographs representative of the morphology of the surface of the samples before and after the polarisation tests are presented. These samples refer to those showing a less steep increase in corrosion currents with the increase in nitrogen content (30 and 52 at % N). Also, the surface morphology of the sample presenting a higher corrosion rate (50 at% N) is presented in the figure. The observed morphology is in good agreement with the results presented in Fig. 4. As a result of the polarization test, pitting was found in all samples. As shown (see Fig. 5g)), pitting is likely to expose the Ti adhesion layer and

the substrate to the solution. Consequently, galvanic effects, which may have a catastrophic effect on the substrate, may arise due to the contact of the substrate, possessing a more negative potential, with both the Ti adhesion layer and the TiN coating which have a more noble potential [13]. However, the amount of pitting is strongly influenced by the amount of nitrogen in the film, or, by other words, increases together with the i_{corr} value. Another important remark is related to the grain size of films. As it can be seen in Fig. 5, thinner structures (30 at%N and 52 at%N; Figs. 5 a) and 5 c), respectively), have shown lower corrosion rates (Fig. 4) and, accordingly, a lower amount of pitting (Figs. 5 d) and 5f)). Conversely, if the columnar structure is less dense, and the grain size is higher (50 at%N, Fig. 5 b)), the corrosion rate will increase.

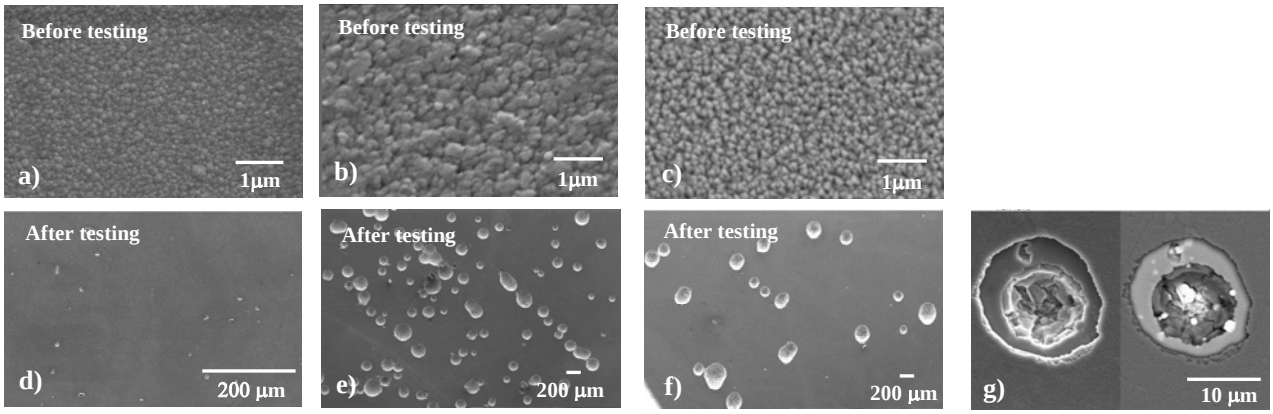

Fig. 5. SEM micrographics obtained for some typical TiNx films before and after polarisation test in artificial sweat solution. a) and d) 30 at.% N; b) and e) 50 at.% N; c) and f) 52 at.% N; g) Pitting in TiNx film

In Fig. 6 the polarisation resistance estimated from the results of the EIS experiments are plotted. Each curve refers to a determined immersion time. Measurements were performed after 1, 2 and 3 days of immersion. The polarization resistance (R_p) is an electrochemical parameter inversely proportional to the corrosion rate. Thus, for comparison, the i_{corr} values obtained from the anodic polarisation experiments are also plotted in the graph (please note that the i_{corr} axis in the graph starts at 1 $\mu A.cm^{-2}$). The estimation of the R_p was calculated by the sum of the substrate polarisation resistance (R_{ps}) and the film polarisation resistance (R_{pf}), according to the method described by *Liu et al.* [14]. Equivalent circuit models were simulated in order to allow the deduction of R_{ps} and R_{pf} values. A very good agreement between the fitted and experimental data was always obtained.

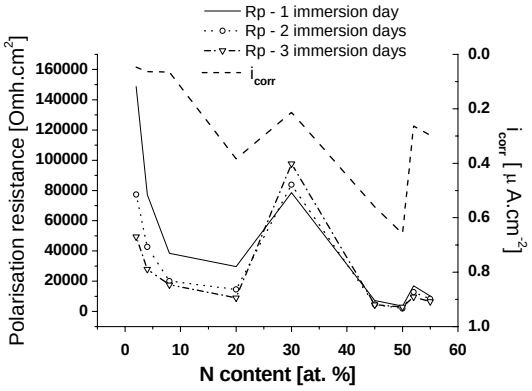

Fig. 6. Influence of the nitrogen amount and immersion time on polarisation resistance of the samples. For comparison, the evolution of i_{corr} with the nitrogen content is also plotted in the graph.

Both high R_{ps} and R_{pf} values were obtained at low immersion times (1 day), in the samples containing low amounts of nitrogen, resulting in an overall high polarisation resistance. However, data plotted in Fig. 6 shows that polarisation resistance is strongly reduced when the immersion time increases up to 3 days, this being an indication of the detrimental effect of the solution on the characteristics of the film. Similar behaviour was found in the samples with less than 30% of N. In fact, the 30 at% N film presents an opposite

behaviour, i.e., both R_{ps} and R_{pf} significantly rises with the immersion time. Finally, the polarisation resistance of the samples with higher nitrogen amounts appears to almost independent of the immersion time, this being an indication of a high stability of the coatings when in contact with the solution.

Thus, the superior corrosion resistance of the films with less than 8 at% N may be attributed to the presence of significant amounts of α-Ti phase and the dense structure detected by SEM observations. Also, these samples exhibited higher film thickness (between 3.8 and 4.2 μm) than the other films.

As referred above the evolution of the α-Ti phase to the ε-Ti_2N occurring in the 20 and 30 at % N films is accompanied by a grain refining effect. In addition, the 30% at% N, although presenting a relatively low thickness (ca. 2.9 μm), is also characterised by a very dense structure which is likely to explain its high corrosion resistance.

Finally, the better corrosion resistance of films containing 52 and 55 at% of N, when compared with films with 45 and 50 at% of N, may be related to the tendency of the columnar structure of the films to become denser as the N content increases. In fact, this increase in column density contributes to a decrease in the surface roughness, as confirmed by SEM observations, and creates a barrier for the diffusion of the electrolyte in direction to the substrate. Nevertheless, the low thickness (1.7 to 1.9 μm) of the coatings with N contents higher than 45%, may explain the lower polarisation resistance of these films when compared with to those containing less amount of N.

Conclusions

The corrosion behaviour of substoichiometric TiN films was investigated by potentiodynamic polarisation and electrochemical impedance spectroscopy. The best corrosion behaviour was obtained in the TiN films containing low percentages of N, i.e. in which an α-Ti phase is present, characterised by a dense structure.
The TiN films close to the stoichiometric condition revealed the lowest corrosion resistance, most probably because an inferior coating thickness. Even so, in these samples it was possible to observe that the corrosion behaviour is influenced by the characteristics of the columnar structure of the film, which is likely to make more difficult the diffusion of the solution species down to the substrate.
A relatively high corrosion resistance was found in the 30 at% N sample, which was attributed to the fine-grained and compact structure characteristic of this sample. In addition, the 30 at% N film presents a very high hardness, which makes it a promising solution for situations in which high corrosion and wear resistances are required.

Acknowledgements

The authors acknowledge the financial support provided by Fundação para a Ciência e a Tecnologia (FCT-Portugal) to E. Ariza through the contract SFRH/BPD/5518/2001.

References

[1] D. A. Glocker, S. I. Shah: Handbook of Thin Film Process Technology, IOP Publishing, Bristol and Philadelphia, Vol. 2, 1995
[2] H. Randhawa: Surf. Coat. Technol. Vol. 36 (1988), p. 829
[3] T. Takagi: Thin Sol. Films Vol 92 (1982), p. 1
[4] D. N. Lee: Journal of Materials Science Vol. 24 (1989), p. 4375
[5] M. J. Brett : J. Vac. Sci. Technol. Vol. A6 (3) (1988), p.1749
[6] F. Elstner, A. Ehrlich, H. Giegengack, H. Kupfer, F. Richter: J. Vac. Sc. Techn. A Vol. 12 (1994), p. 476
[7] G. Berg, C. Friedrich, E. Broszeit, K.H. Kloos: Surf. Coat. Techn. Vol. 74-75 (1995), p. 135
[8] M. Kawamura, Y. Abe, H. Yanagisawa, K. Sasaki: Thin Sol. Films Vol. 287 (1996), p.115
[9] E. Ribeiro, A. Malczyk, S. Carvalho, L. Rebouta, J. V. Fernandes, E. Alves, A. S. Miranda: Surf. Coat. Technol. Vol 151-152 (2002), p. 515
[10] J. Kohlscheen, H.-R. Stock, P. Mayr: Surf. Coat. Technol. Vol 120-121 (1999), p. 740
[11] S. Yang, D. B. Lewis, I. Wadsworth, J. Cawley, J. S. Brooks and W. D. Münz: Surf. Coat. Technol. Vol 131 (2000), p. 228
[12] J. -H. Huang, Y. -P. Tsai and G. -P. Yu: Thin Sol. Films Vol. 355-356 (1999), p. 440
[13] C. V. Franco, L. C. Fontana, D. Bechi, A. E. Martinelli and J. L. R. Muzart: Corr. Sci. Vol. 40 (1998), p. 103
[14] C. Liu, A. Leyand, Q. Bi, A. Matthews: Surf. Coat. Technol. Vol. 141 (2001), p. 164